Adaptive Illumination Estimation for Low-Light Image Enhancement

Lan Li, Wen-Hao Peng, Zhao-Peng Duan and Sha-Sha Pu

***Abstract*—In order to obtain accurate information from low illumination images, we propose a low-light image enhancement method based on guided filter and Gamma correction according to the Retinex model. First, the image is converted into the Lab color space. After that, the guided filter is used to extract the scene's illumination and the parameter of local square window radius is updated by the size of source image. Then, a novel adaptive Gamma correction, based on heat transfer law, is applied to achieve precise illumination intensity. Finally, the illumination component with color information is to obtain the reconstructed enhancement image. The ablation analysis indicates the effectiveness of main part in the proposed method. Through numerous experiments, the proposed method enhances the overall brightness, corrects the color distortion, preserves details, and demonstrates favorable visual results for diverse low-light images. The proposed method also shows certain superiority and comparability in objective and subjective evaluations compared to state-of-the-art methods, and meanwhile remains highly efficient.**

***Index Terms*—Retinex, guided filter, Gamma correction, color correction, image enhancement**

I. Introduction

Uneven and insufficient lighting circumstances, such as at night or on cloudy days, can hinder the effective capture of information [1]-[2]. As a result, it can cause difficulties in extracting and processing information. In low-light scenes, the sensitivity of the imaging system sensor is limited due to device property, and only the fewer photons are obtained by imaging system, these lead to low contrast and the color distortion in acquired images [3]-[4]. Images taken in low light typically present shortcomings including low brightness and poor visual effect. Fig. 1 displays three original low-light images and the corresponding enhanced outcomes. It is evident from the Fig. 1 that the processed images illustrate information more effectively than the originals. Low-light image enhancement has been widely used, including mine image [5].

(a) Images with low-light.

(b) Corresponding outcomes by the proposed method.

Fig. 1. Example of low-light image enhancement.

Various methods have been devised to execute the enhanced tasks. Histogram equalization (HE) [6] is one of the most typical brightness adjustment method. HE enhances contrast and expending dynamic range by redistributing the probability density of grayscale values [7]. Nonetheless, HE intensifies noise in dark areas by incorporating lower grey values and is prone to artifact generation due to its disregard for the image's local features. Adaptive histogram equalization (AHE) [8] divides the image into blocks to concentrate on local contrast enhancement. However, the outputs often exhibit block effects, and the challenges still exist. Pisano et al. [9] introduced contrast limited adaptive histogram equalization (CLAHE), which utilizes interpolation to circumvent block effects and suppress noise. Although HE-based methods typically excel in enhancing brightness, they are not effective in enhancing color images, and reconstructed outputs tend to be flawed due to artifacts.

Nonlinear mapping methods represent another category in the field of image enhancement. They aim to achieve specific goals by means of tailor-made functions. The Gamma function can adjust the brightness in low-light images process, which is commonly known as Gamma Correction (GC). However, GC often over-enhances the images and amplifies noise by using invariant parameters. Adaptive Gamma correction with weighting distribution (AGCWD) is introduced in [10]. This method utilizes a weight histogram to compute the Gamma values to ensure contrast improvement. The homomorphic filter (HF) [11] is a standard image enhancement method relying on domain transfer functions. HF decomposes the images into low and high frequency components. These components are averaged and logarithmically transformed, respectively. These steps aim to improve brightness and contrast, and eliminate noise. However, HF's drawback is its tendency to blur detail information. While nonlinear mapping methods can enhance

Manuscript received August 3, 2023; revised January 8, 2024.

This work was supported by Natural Science Basic Program of Shaanxi (Project No. 2021JM-399), the Graduate Innovation and Practical Ability Training Project of Xi'an Shiyou University (YCS22213180).

Lan Li is a professor of School of Science, Xi'an Shiyou University, Xi'an, Shaanxi, CO 710065, China. (Corresponding author to provide phone: 86+029-88382735, e-mail: lanli@xsyu.edu.cn).

Wen-Hao Peng is a postgraduate student of School of Science, Xi'an Shiyou University, Xi'an, Shaanxi, CO 710065, China. (e-mail: wilson_peng2021@163.com).

Zhao-Peng Duan is a postgraduate student of School of Science, Xi'an Shiyou University, Xi'an, Shaanxi, CO 710065, China. (e-mail: 2394942440 @qq.com).

Sha-Sha Pu is a postgraduate student of School of Science, Xi'an Shiyou University, Xi'an, Shaanxi, CO 710065, China. (e-mail: pushashay@163.com).

images, the basic mapping functions are unsuitable for complex low-light images.

As machine learning evolves, researchers are trying to find a more appropriate mapping relationships for low-light image enhancement from various datasets [12]-[13]. These methods incorporate a series of modules to extract attributes, culminating in enhanced outputs through extensive encoding, decoding and reconstruction processes. Wei et al. [14] introduced Retinex-Net to enhance images and construct a large dataset. Retinex-Net is end-to-end trainable, and the outputs preserve the main structures while distort the color. Kind++ [15] offers superior natural color, but compromises image detail and structure. These methods do not perform well on natural images due to the lack of large datasets, and data training is time consuming and requires expensive hardware devices support.

For natural low-light image enhancement, the perceptual imaging model-based methods attract considerable attention [16]-[17]. These methods, derived from the human retina perception system, divide images into the components about illumination and reflectance, with subsequent operations aimed at these elements. Representative methods include single scale Retinex (SSR), multi scale Retinex (MSR) [18] and multi scale Retinex with color restoration (MSRCR) [19]. The naturalness preserved enhancement (NPE) method [20], which focuses local brightness, contrast enhancement, and overall natural preservation, can achieve superior image reconstructed results. However, this method may have difficulties in brighter regions. The simultaneous reflection and illumination estimation (SRIE) method [21] includes a weighted variation model to enhance image quality, although it may lead to the creation of artifacts in edge structure. Li et al. [22] proposed a robust Retinex model to reduce noise. The model utilizes an iterative algorithm for optimization. Nevertheless, this can be time-consuming and may exclude details in dark regions. Wu et al. [23] leveraged a 2D histogram to amplify reflection components, specifically reflectance oriented probabilistic equalization (ROPE) method. However, it has tendency to over-enhance images.

To achieve high-quality image output with minimal artifacts and color distortion, this paper proposes a low-light image enhancement method. Through the perception of image information, the method automatically obtains corresponding parameters, and effectively improves the image visual effect. The low-light image is constructed with high contrast, vivid color and intricate details via proposed method. Compared with previous methods, this paper has the following contributions.

1. In the illuminance estimation process, the parameter r is set by the image size, and the appropriate guided filter is obtained adaptively.

2. To achieve precise light intensity, we have designed an adaptive strategy for selecting parameter γ. This strategy is driven by the local and global information perceived in the input image. This approach ensures accurate illumination estimation in accordance with the heat transfer law.

The rest of the paper is organized as follows: Section II outlines the pertinent models and methods. Section III provides details exposition of the proposed method. Section IV and Section V present the experimental analysis and conclusions, respectively.

II. Related Works

A. Retinex Model

The Retinex model comes from the human vision imaging system, and is widely utilized due to its simplicity. It can be formulated as Eq. (1):

$$S = L \bullet R, \tag{1}$$

where S is the source image, L is illuminance distribution of surroundings, and R is the target enhanced scene, the operator '$\bullet$' indicates element-wise multiplication.

B. The Guided Filter

The guided filter [24] is a filter that has the local linear model as a basis. In comparison to the nonlinear filter, it has a reduced calculation complexity. Within a k-centered window ω_k, the relationship of the output image q and the guided image I is linear, we have,

$$q(i,j) = a_k I(i,j) + b_k,\ \forall (i,j) \in \omega_k, \tag{2}$$

where (i,j) and k are pixel indexes, a_k and b_k are the coefficients of linear equation, respectively. In Eq. (2), if I equals input image p, the guided filter can be utilized as an edge-preserving filter. Thus, we obtain,

$$\begin{cases} a_k = \dfrac{\sigma_k^2}{\sigma_k^2 + \varepsilon} \\ b_k = (1 - a_k)\overline{p}_k \end{cases}, \tag{3}$$

where σ_k^2 and $\overline{p}_k$ are the variance and mean of p within window ω_k, respectively. ε is a constant. In Eq. (3), the parameter a_k is in $[0,1]$, and significantly impacts the output. By altering the size of filter windows, both the overall and local smooth effect of image is affected, and distinct levels of structure and texture information are retained.

C. Gamma Correction

GC is a widely employed technique for enhancing image. It alters the image's brightness and contrast via non-linear transformation, and augments its detail and sharpness. The canonical form for expressing this is as follows,

$$O = L^{\gamma},\quad \gamma > 0, \tag{4}$$

where O is the corrected image, L is the input image, and γ is the correction parameter to change the image brightness. The image is darkened for $\gamma > 1$, and brightened for $\gamma < 1$, $\gamma = 1$ does not give changes.

III. Adaptive Illumination Estimation and Image Reconstruction

Fig. 2 displays the flow chart of the proposed method.

A. Conversion of RGB to Lab

The transformation of color images in RGB can cause distortion due to the strong color correlation inherent in RGB space. The Lab space, on the other hand, separates the brightness information into the L-layer map and the color information into the a- and b-layer maps. As these maps are independent of each other, changing the L map does not

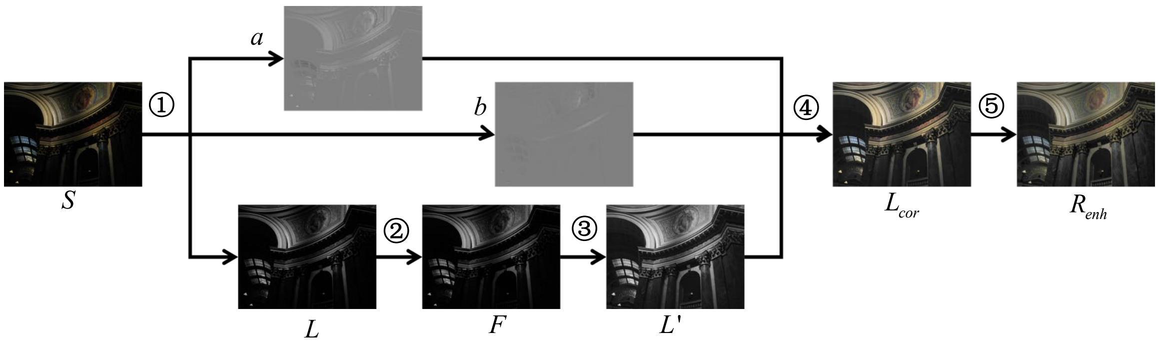

① RGB to Lab; ② Illumination estimation; ③ Adaptive illumination intensity correction; ④ Lab to RGB; ⑤ Image reconstruction

Fig. 2. A flow chart of the proposed method.

create new color information. Therefore, we convert images from RGB to Lab for further research. The formula for converting RGB to XYZ space is as follows,

$$\begin{cases} X = 0.433953R + 0.376219G + 0.189828B \\ Y = 0.212671R + 0.715160G + 0.072169B \\ Z = 0.017758R + 0.109477G + 0.872865B \end{cases}, \tag{5}$$

where the R, G and B are the components of RGB color space, their values fall within the range of 0 to 1. Meanwhile, the values of X, Y and Z represent the three channels of the XYZ color space, respectively. The following formulas are the conversion of XYZ to Lab,

$$\begin{cases} L = 116 f(Y) - 16 \\ a = 500[f(X) - f(Y)], \\ b = 200[f(Y) - f(Z)] \end{cases} \tag{6}$$

and

$$f(t) = \begin{cases} t^{1/3} & t > (\frac{6}{29})^3 \\ \frac{1}{3}(\frac{29}{6})^2 t + \frac{4}{29} & otherwise \end{cases}, \tag{7}$$

B. Illuminance Estimation

The intensity of light changes slowly in the local space from the optical imaging process. During illumination extraction, the elimination of extraneous details that are present in the input image is crucial. Additionally, optical imaging projects 3-D spatial information onto a 2-D plane, which can make objects close together in the image but they appear far apart in the reality, so it is critical to preserve structural information with spatial properties.

As outlined in Section II, the guided filter is a linear filter that can effectively retain edge information. For the luminance layer map L, the estimated map for illuminance F can be obtained by:

$$F = G(L, O, r), \tag{8}$$

where $G(\bullet)$ represents the guided filter operator, O denotes the guiding image, and r is the local square window radius. To ensure the filter's edge protection capability, it is typically recommended to set O equal to L.

During guided filtering, a larger local square window size results the filter to focus more on general contour of the images, which can cause heavy loss of information. Therefore, it is crucial to carefully choose an appropriate size of the local square window. After several experiments, the local square window radius is selected by $r = round((r_1 + r_2)/2)$, where $r_1 = round(\min(h, w)/8)$, $r_2 = round(\min(h, w)/2 - 1)$, h and w denote the input image length and width, respectively, and $round(\bullet)$ is a round operation.

C. Adaptive Illumination Intensity Correction

When the light travels from the source to the acquisition device, its intensity decreases, and this is not linear. Due to its non-linear characteristic, GC is commonly employed to regulate the grayscale values. In this paper, the GC format can be presented as,

$$L' = 100 \times \left(\frac{F}{100} \right)^{\gamma}, \tag{9}$$

where L' is the illumination corrected map, F is estimated illuminance map from L, γ lies between (0, 1).

From Eq. (9), it is apparent that a fixed parameter is a crude strategy for selecting γ and is not suitable for different images. According to the laws of heat transfer, an object with higher energy will radiate energy to its surroundings unconsciously. Simultaneously, the greater the energy difference between the object and its surroundings, the faster its energy decay rate. Similar laws apply to optical propagation. Thus, we design a new strategy to correct illuminance intensity in finding the suitable γ. The formula for this strategy can be represented as follows,

$$\gamma = \frac{1}{1 + \exp(F')}, \tag{10}$$

and

$$F' = (F - F_{\min})/(F_{\max} - F_{\min}), \tag{11}$$

where $F_{\max}$ and $F_{\min}$ are the maximum and minimum values of F, respectively. As the F value increases, the smaller γ becomes, the L' is brighter.

D. Conversion of Lab to RGB

After obtaining the corrected intensity map L', it is merged with the initial *a*- and *b*-layers to produce a new image. Then, it is converted into RGB to obtain the needed estimated illumination component L_{cor}. The conversion of Lab to RGB color space is outlined as follows,

$$\begin{cases} Y' = f^{-1}[(L'+16)/116] \\ X' = f^{-1}[(L'+16)/116 + a/500], \\ Z' = f^{-1}[(L'+16)/116 - b/200] \end{cases} \tag{12}$$

where X', Y' and Z' are new layers in XYZ color space, and

$$f^{-1}(t)=\begin{cases} t^3 & t>\frac{4}{29} \\ 3\left(\frac{6}{29}\right)^2\left(t-\frac{4}{29}\right) & otherwise \end{cases} \quad (13)$$

The XYZ space is converted to RGB by,

$$\begin{cases} R'=3.0799327X'-1.537150Y'+0.542782Z' \\ G'=-0.921235X'+1.875992Y'+0.0452442Z', \\ B'=0.0528909X'-0.204043Y'+1.1511515Z' \end{cases} \quad (14)$$

where R', G' and B' are components of L_{cor} in RGB color space.

E. Image Reconstruction

The reconstructed enhancement image R_{enh} is achieved by substituting L_{cor} into Eq. (15).

$$R_{enh}=S/\left(L_{cor}+eps\right), \quad (15)$$

where S is the source image, eps is a minimum constant, and L_{cor} includes the property of scenarios, such as non-uniform luminance and color temperature, among others. As a result, the enhanced image is reconstructed without any of the negative effects by the scenario light.

F. Ablation Analysis

Here, we present the intermediate outcomes of the proposed method, and explain the significance of the main part of the proposed method through ablation analysis.

(a) (b) (c)

Fig. 3. Intermediate result and utility of the proposed method. (a) Original. (b) The illuminance map F via our guided filter. (c) The corrected illuminance map L' by adaptive GC.

(a) (b) (c)

Fig. 4. The color corrected capacity in the proposed method. (a) Original. (b) The illumination component L_{cor}. (c) The reconstructed result by the proposed method.

Fig. 3(b) depicts the illuminance map F, while Fig. 3(c) illustrates the illuminance map L' corrected by the suggested adaptive GC. Generally, L' appears brighter than F. It is readily noticeable that the 'car', 'road' and 'trees' are illuminated at varying degrees in the picture. The image, on the whole, has a wide dynamic range and retains the property of the uneven light distribution. Upon analysis, an accurate illumination estimate is attained.

Fig. 4(b) produces a bright vision effect, but shows serious color deviation. The 'trees' in dark is still hidden. The reconstructed result has corrected color and further improved brightness in Fig. 4(c). Overall, the output image appears clear and is less impacted by ambient light.

(a) (b) (c)

Fig. 5. Enhanced images obtained after estimation in different color space. (a) Original. (b) The estimation in RGB space. (c) The estimation in Lab space.

Form Fig. 5, it can be seen that the proposed method can more effectively enhance the low-light image. Although Fig. 5(b) is brighter than the original, the bright areas of Fig. 5(b) are over-enhanced and the dark areas under-enhanced compared to Fig. 5(c), and the colors are not well reconstructed.

Hence, the aforementioned analysis indicates that the proposed method achieves adaptable estimation and correction, resulting in acquiring improved images.

IV. EXPERIMENTAL RESULTS ANALYSIS

A. Experimental Platform and Datasets

To carry out the experiment, we built a corresponding experimental platform for test, with the help of MATLAB 2018b, the computer processor is i5-7200U CPU @ 2.50 GHz, with 8G RAM, the operating system is Windows10.

To access the efficacy of the proposed method, we have opted to employ a set of low-light images as our experimental datasets. The images are derived from several public datasets, including LIME [25], ExDark [26] and MEF [27], and cover various themes, ranging from human landscapes to natural views and even animals.

Some low-light images have been randomly selected from ExDark as experimental samples and are depicted in Fig. 6. The corresponding enhanced outcomes obtained by the proposed method can be viewed in Fig. 7. The enhanced images exhibit well-exposed features, natural color, boosted contrast and visibility of dark areas, and clear and abundant details.

B. Subjective Evaluation

(1) Comparison with traditional enhancement methods

In this section, we compare experimental results of 5 traditional enhancement methods and ours. The traditional methods are CLAHE [9], HE [6], MSR [18], MSRCR [19], HF [11]. Fig. 8, 9 and 10 show results of these methods.

Fig. 8 shows the results of enhancing image X_1. Image X_1 is a low-light image under uneven lighting. As can be seen from the flowers, wall and cup that CLAHE and HE enhance the noise of the image. The results of HE, MSR and MSRCR have an over- amplification of brightness with a consequent loss of detail and structure. The results of CLAHE and HF do not gain a global increase in brightness. The proposed method increases the brightness in a balanced way and reduces the effect of uneven illumination in the image. For image X_2, the CLAHE result has noticeable artefacts and color distortion. HE, MSR and MSRCR produce results with sky color distortion. HF and the proposed method both produce undistorted results, but the HF result is dark. For image X_3, the result obtained by our method has retained the clear and rich structure and detail.

Fig. 6. Some experimental samples of low-light images.

Fig. 7. Corresponding enhancement results by the proposed method.

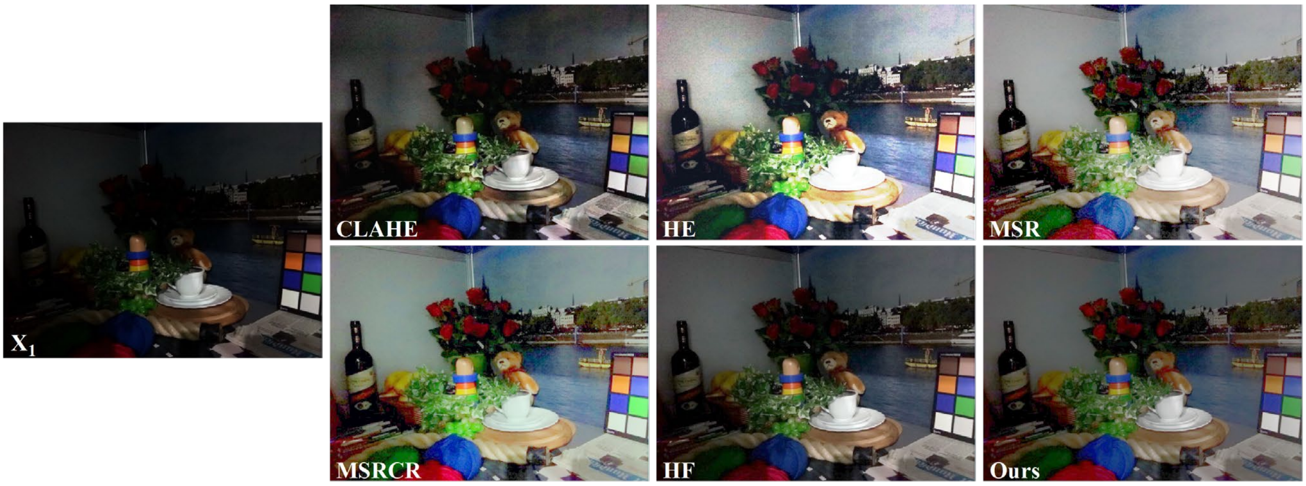

Fig. 8. Comparison results with traditional enhancement methods. Image X_1 is taken from LIME dataset.

Fig. 9. Comparison results with traditional enhancement methods. Image X_2 is taken from ExDark dataset.

(2) Comparison with the state-of-the-art enhancement methods

Fig. 11 shows the results of 4 real-life image processed by state-of-the-art methods and ours. The state-of-the-art methods are AGCWD [10], NPE [20], Robust Retinex [22], SIRE [21], ROPE [23], Retinex-Net [14], and Kind++ [15]. The image X_4 is taken from Exdark dataset, is a nighttime image. Image X_5, X_6 and X_7 are taken from MEF dataset. X_5 is a low-light image with backlighting, X_6 is a low-light image with uneven lighting, X_7 is a low-light image with backlighting and color distortion.

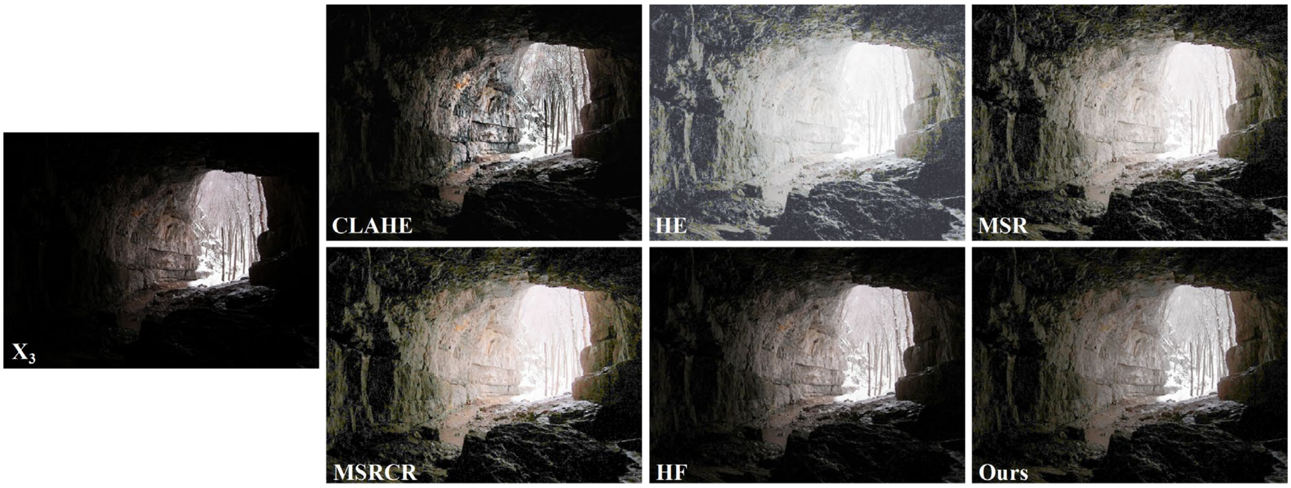

Fig. 10. Comparison results with traditional enhancement methods. Image X_3 is taken from MEF dataset.

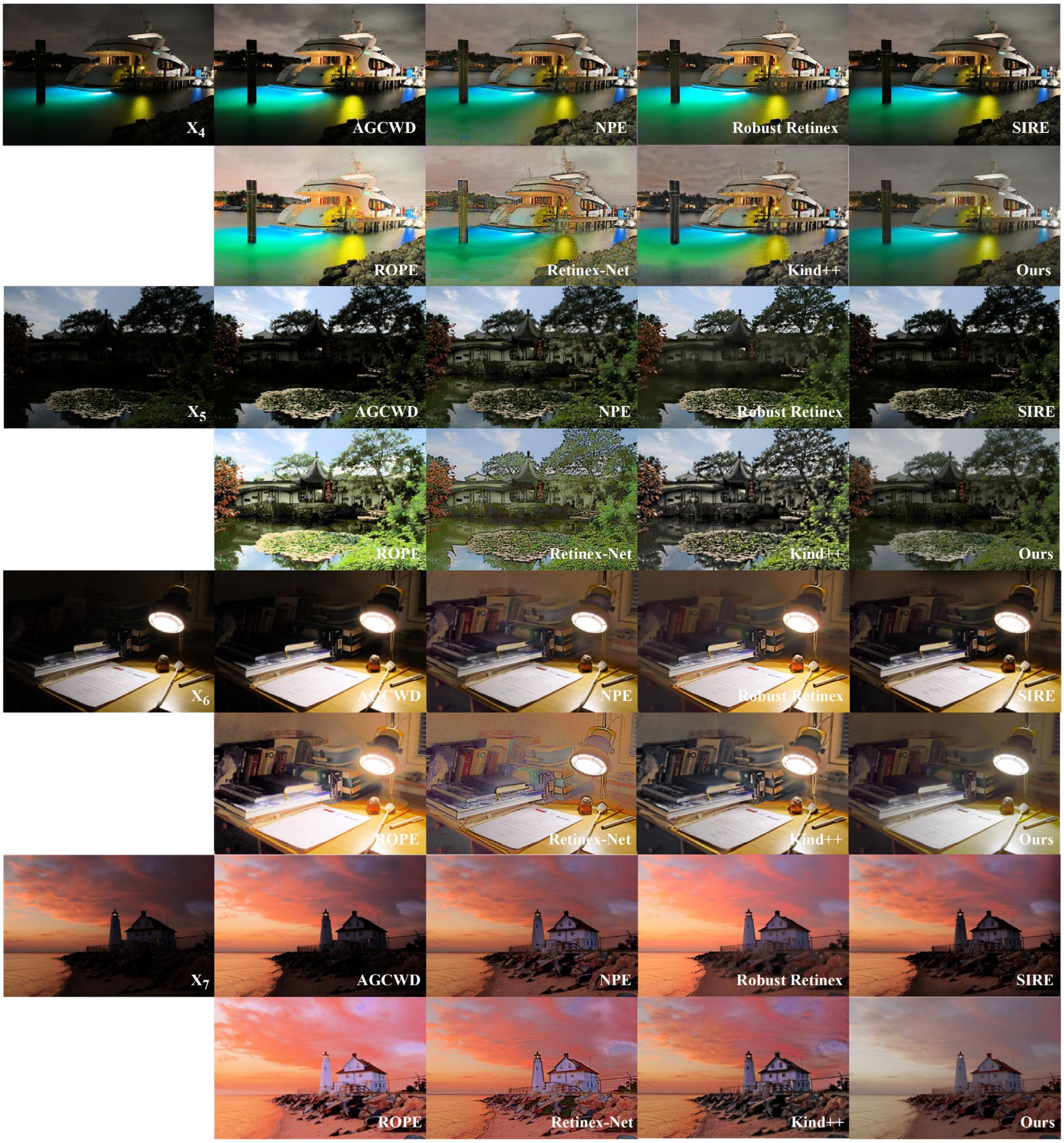

Fig. 11. Comparison results with state-of-the-art enhancement methods. Image X_4 is taken from ExDark dataset. Image X_5, X_6 and X_7 are taken from MEF dataset.

Fig. 12. Comparison results of image pairs with state-of-the-art enhancement methods. Image X_8, X_9, X_{10}, X_{11} and synthetics are taken from IEC dataset.

From the results in Fig. 11, the AGCWD seems to give minimal improvement of brightness as the images remain dark. On the other hand, the NPE brightens the images, but contains structural artifacts and noise in shaded areas, as in image X_4. The Robust Retinex can enhance brightness of the images but it blurs the details. For example, from the result of image X_4 and X_6, the recognition of details is reduced. SIRE preserves the naturalness of the bright areas, with less enhancement in the darker areas, and retains dark edge artifacts in image X_4 and X_6. The images produced by ROPE are the brightest. However, they are over-enhanced and noisy. For the machine learning based methods, Retinex-Net enhances the brightness of images, but the outcomes appear to be afflicted with color distortion and halo artifacts in image X_4 and X_7. Similarly, Kind++ produces artifacts in the bright areas even though contrast is improved in darker areas. The proposed method is capable of emphasizing the intricacies and refining darker color without excessive enhancement, resulting in a more authentic and clearer presentation.

To further investigate the effects of these methods of enhancement, we also carry out experiments utilizing the image pairs from IEC database [28] and Fig. 12 presents the corresponding results. The Fig. 12 shows that the brightness of the results obtained from AGCWD and SIRE is lower than that of the reference images. Additionally, NPE and Robust Retinex cause loss of details. The brightness of the ROPE results surpasses that of synthetic images. For the machine learning results, both Retinex-Net and Kind++ exhibit serious distortions and artifacts. The results produced by the proposed method bear a closer resemblance to reference

TABLE I
AVERAGE SCORE OF BRISQUE ↓ ON DIFFERENT DATASETS.

Method	AGCWD	NPE	Robust Retinex	SIRE	ROPE	Retinex-Net	Kind++	Ours
ExDark	22.26	23.11	<u>21.14</u>	23.9	24.17	24.43	25.98	**19.57**
MEF	31.78	27.87	30.41	<u>24.61</u>	27.62	22.94	32.36	**21.42**
IEC	28.13	<u>23.04</u>	29.8	26.95	**22.88**	42.67	42.91	30.78
Average	28.13	<u>24.67</u>	27.12	25.16	24.89	30.01	33.75	**23.92**

TABLE II
AVERAGE SCORE OF NIQE ↓ ON DIFFERENT DATASETS.

Method	AGCWD	NPE	Robust Retinex	SIRE	ROPE	Retinex-Net	Kind++	Ours
ExDark	**2.98**	3.3	3.81	<u>3.2</u>	3.35	4.11	3.78	3.24
MEF	3.06	<u>2.53</u>	3.73	2.65	2.81	3.19	2.86	**2.32**
IEC	<u>2.19</u>	**2.11**	2.7	2.28	2.39	4.33	3.94	2.61
Average	2.75	**2.64**	3.41	<u>2.71</u>	2.85	3.88	3.53	2.72

TABLE III
AVERAGE SCORE OF LOE ↓ ON DIFFERENT DATASETS.

Method	AGCWD	NPE	Robust Retinex	SIRE	ROPE	Retinex-Net	Kind++	Ours
ExDark	**77.28**	524.46	414.99	384.15	171.06	879.66	526.05	<u>164.61</u>
MEF	**73.46**	383.39	243.66	259.95	178	590.45	241.98	<u>133.86</u>
IEC	**50.06**	476.15	192.71	279.84	169.12	776.78	503.66	<u>132.49</u>
Average	**66.94**	461.33	283.78	307.98	172.72	748.96	423.9	<u>143.65</u>

TABLE IV
RUNNING TIME OF DIFFERENT METHODS ON DIFFERENT SIZE IMAGES (UNIT: SECONDS).

Method	Image sizes				
	384×384×3 pixels	600×530×3 pixels	800×530×3 pixels	1280×960×3 pixels	2304×1728×3 pixels
MSR	**0.16**	**0.32**	**0.48**	<u>1.13</u>	**3.96**
MSRCR	<u>0.19</u>	<u>0.34</u>	0.55	1.27	4.59
NPE	5.35	9.67	15.12	24.68	142.58
Robust Retinex	8.68	16.49	60.27	78.34	-
SIRE	8.02	10.08	32.92	52.45	998.79
ROPE	0.58	0.69	0.87	1.15	4.79
Ours	<u>0.19</u>	**0.32**	<u>0.5</u>	**0.83**	<u>4.56</u>

images than those generated by state-of-the-art methods, with a consistent color representation.

Overall, the proposed method is consistent with the human visual system, effectively correcting color distortion whilst maintaining naturalness and detail. Most importantly, the proposed method notably enhances contrast and visibility in darker areas. In terms of visual quality, the proposed method outperforms the other methods.

C. *Objective Evaluation*

To comprehensively evaluate the performance of different methods, we adopt the objective image quality assessment (IQA) to measure the performance of each. We collect images from ExDark, MEF and IEC datasets to test experimentally. The image quality is assessed using the BRISQUE (blind/referenceless image spatial quality evaluator) [29], NIQE (natural image quality evaluator) [30] and the LOE (lightness order error) [20] assessments.

BRISQUE and NIQE are two commonly used metrics for objectively evaluating image quality without reference, known as no-reference IQA. They use statistical analysis of spatial features in images to obtain an assessment score and measure the intensity of distortion or naturalness of the image, respectively. The lower score for both metrics indicate higher image quality.

The LOE measures the similarity of brightness difference between the source image and reconstructed image, serving as a reduced-reference IQA. A lower LOE value indicates better preservation of the brightness property.

Table I-III display the BRISQUE, NIQE and LOE metrics scores, respectively. Each score is an average over the corresponding dataset. The best values are highlighted in bold and secondary values are underlined.

Table I demonstrates that the proposed method has excellent performance in terms of BRISQUE values, and the average value is minimal. Notably, the values derived from the proposed method are quite smaller than other method in ExDark and MEF datasets. And in Table II, the values of the proposed method are the lowest in MEF datasets, and they are of the medium level on average. Based on Table I and II, the proposed method has shown some advantages in enhancing naturalness of the image. According to the LOE values displayed in Table III, the AGCWD method exhibits the best performance owing to its minimal increase in brightness, whereas the proposed method demonstrates the second-best performance in all the datasets. Table III reveals that the proposed method has a high capability retaining image properties. Overall, the proposed method is both comparable and superior.

D. *Running Time*

In this part, we conduce a series of tests on images of various sizes to determine the running time of the proposed method and several Retinex-based methods on the same platform. The time cost of each method is presented in Table IV. We repeat the test 10 times for each image and calculate the average time cost for image enhancement using different methods. As outlined in Table IV, the proposed method offers certain advantages over other Retinex-based methods.

After thorough analysis, it has been concluded that the conversion from Lab to RGB color space is a time-intensive process. As depicted in Fig. 13, the enhancement of a

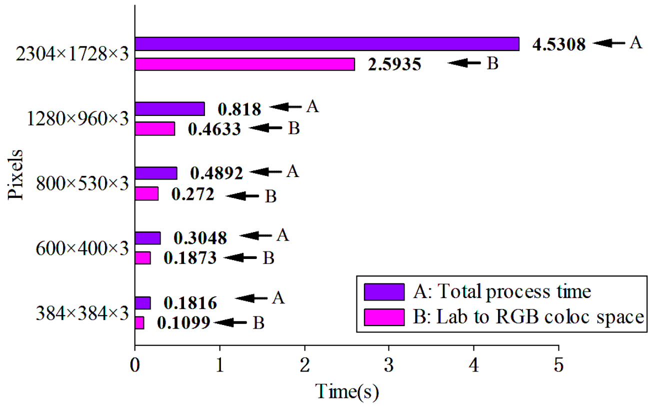

Fig. 13. Running time of different step in the proposed method.

2304×1728×3 pixels image requires 4.5308s while inverse color space conversion takes 2.5935s. The proposed method takes 0.818s, 0.4892s, 0.3048s and 0.1816s to enhance images of 1280×960×3, 800×530×3, 600×400×3 and 384×384×3 pixels, respectively. However, it takes 0.4633s, 0.272s, 0.1873s and 0.1099s to convert from Lab to RGB color space, respectively. Therefore, the improvement of the efficiency of Lab to RGB is essential to speed up the proposed method.

E. Failure cases

In further experiment, there is a noise amplification of the noisy images. Fig. 14 shows some examples of images with ISO noise. The visual effect appears foggy due to the retained and amplified noise, despite the increased brightness of the banana, dog, and shoe. This is mainly due to the fact that the potential ISO noise occupies a relatively large proportion of the image, and the noise distribution is irregular and difficult to distinguish. It is therefore a difficult problem to enhance low-light images with significant noise.

(a) Source noisy images

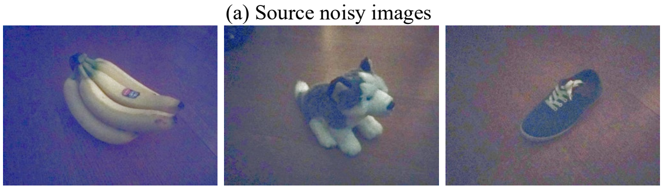

(b) Corresponding enhancement of noisy images

Fig. 14. Examples of noisy image enhancement.

V. Conclusion

In this paper, we present a novel method to enhance the images with low-light by using doubly adaptive strategy and Retinex model. First, the image is converted to Lab color space to eliminate the strong correlated relation between color information in RGB space. The L-layer map is then used as initial estimator of the illumination intensity component, and the corrected component is then obtained by using adaptive guided filter and GC. To further wipe off the detrimental effects from unfavorable lighting conditions, the corrected color illumination component is incorporated into Retinex model to enhance images. Numerous experiments indicate that the proposed method brightens image, corrects color deviation, and provides more natural looking reconstructed results. The comparative experimental results illustrate the advantages and comparison of the proposed method. Upon further analysis, it has become apparent that the processing of color space conversion consumes significant amount of time. Therefore, it is necessary to reduce the complexity of the conversion in the future. Additionally, the denoising in low-light image enhancement is also a challenging problem.

References

[1] L. Ma, T. Y. Ma, R. and S. Liu, "The review of low-light image enhancement," Journal of Image and Graphics, vol. 27, no. 5, pp. 1392-1409, 2022.

[2] M. T. Rasheed, G. Guo, D. Shi, H. Khan, and X. Cheng, "An empirical study on retinex methods for low-light image enhancement," Remote Sensing, vol. 14, no. 18, pp. 4608-1-4608-25, 2022.

[3] W. Wang, X. Wu, X. Yuan and Z. Gao, "An experiment-based review of low-light image enhancement methods," IEEE Access, vol. 8, pp. 87884-87917, 2020.

[4] W. Kim, "Low-light image enhancement: a comparative review and prospects," IEEE Access, vol. 10, pp. 84535-84557, 2022.

[5] Y. Wang, H. Wu, Y. Duan, and Z. Li, "An enhancement algorithm of mine image based on adaptive transmittance and hierarchical threshold function," IAENG International Journal of Computer Science, vol. 50, no. 2, pp. 459-467, 2023.

[6] R. Hummel, "Image enhancement by histogram transformation," Computer Graphics and Image Processing, vol. 6, no. 2, pp. 184-195, 1977.

[7] Z. Saberi, N. Hashim, A. Ali, P. Boursier, J. Abdullah, and Z. C. Embi, "Adaptive contrast enhancement of satellite images based on histogram and non-linear transfer function methods," IAENG International Journal of Applied Mathematics, vol. 53, no.1, pp. 341-349, 2023.

[8] T. K. Kim, J. K. Paik and B. S. Kang, "Contrast enhancement system using spatially adaptive histogram equalization with temporal filtering," IEEE Transactions on Consumer Electronics, vol. 44, no. 1, pp. 82-87, 1998.

[9] E. D. Pisano, S. Zong, B. M. Hemminger, M. DeLuca, R. E. Johnston, K. Muller, et al, "Contrast limited adaptive histogram equalization image processing to improve the detection of simulated spiculations in dense mammograms," Journal of Digital Imaging, vol. 11, pp. 193-200, 1998.

[10] S. C. Huang, F. C. Cheng and Y. S. Chiu, "Efficient contrast enhancement using adaptive gamma correction with weighting distribution," IEEE Transactions on Image Processing, vol. 22, no. 3, pp. 1032-1041, 2013.

[11] R. King, M. Ahmadi, R. Gorgui-Naguib, A. Kwabwe, and M. Azimi-Sadjadi, *Digital Filtering in One and Two Dimensions: Design and Applications*. New York: Plenum-Press, 1989, ch. 10.

[12] C. Li, C. Guo, L. Han, J. Jiang, M. Cheng, J. Gu, et al., "Low-light image and video enhancement using deep learning: a survey," IEEE Transactions on Pattern Analysis and Machine Intelligence, vol. 44, no. 12, pp. 9396-9416, 2022.

[13] H. Wu, Y. Qu, S. Lin, J. Zhou, R. Qiao, Z. Zhang, et al, "Contrastive learning for compact single image dehazing," IEEE/CVF Conference on Computer Vision and Pattern Recognition, Montreal, 2021, pp. 10551-10560.

[14] C Wei, W Wang, W Yang and J Liu, "Deep retinex decomposition for low-light enhancement," British Machine Vison Conference, Newcastle, UK, 2018, pp. 1-12.

[15] Y. Zhang, X. Guo, J. Ma, W. Liu, and J. Zhang, "Beyond brightening low-light images," International Journal of Computer Vision, vol. 129, pp. 1013-1037, 2021.

[16] Z. Fan, C. Tang, Y. Shen, M. Xu, and Z. Lei, "RME: a low-light image enhancement model based on reflectance map enhancing," Signal, Image and Video Processing, vol. 17, no. 4, pp. 1493-1502, 2023.

[17] Z. Al-Ameen, "Nighttime image enhancement using a new illumination boost algorithm," IET Image Processing, vol. 13, no. 2, pp. 1314-1320, 2019.

[18] D. J. Jobson, Z. Rahman and G. A. Woodell, "Properties and performance of a center/surround retinex," IEEE Transactions on Image Processing, vol. 6, no. 3, pp. 451-462, 1997.
[19] D. J. Jobson, Z. Rahman and G. A. Woodell, "A multiscale retinex for bridging the gap between color images and the human observation of scenes," IEEE Transactions on Image Processing, vol. 6, no. 7, pp. 965-976, 1997.
[20] S. Wang, J. Zheng, H. M. Hu and B. Li, "Naturalness preserved enhancement algorithm for non-uniform illumination images," IEEE Transactions on Image Processing, vol. 22, no. 9, pp. 3538-3548, 2013.
[21] X. Fu, D. Zeng, Y. Huang, X. P. Zhang, and X. Ding, "A weighted variational model for simultaneous reflectance and illumination estimation," IEEE Conference on Computer Vision and Pattern Recognition, Las Vegas, 2016, pp. 2782-2790.
[22] M. Li, J. Liu, W. Yang, X. Sun and Z. Guo, "Structure-revealing low-light image enhancement via robust retinex Model," IEEE Transactions on Image Processing, vol. 27, no. 6, pp. 2828-2841, 2018.
[23] X. Wu, Y. Sun, A. Kimura and K. Kashino, "Reflectance-oriented probabilistic equalization for image enhancement," IEEE International Conference on Acoustics, Speech and Signal Processing, Toronto, 2021, pp. 1835-1839.
[24] K. He, J. Sun and X. Tang, "Guided image filtering," IEEE Transactions on Pattern Analysis and Machine Intelligence, vol. 35, no. 6, pp. 1397-1409, 2013.
[25] X. Guo, Y. Li and H. Ling, "LIME: Low-light image enhancement via illumination map estimation," IEEE Transactions on Image Processing, vol. 26, no. 2, pp. 982-993, 2017.
[26] Y. P. Loh, and C. S. Chan, "Getting to know low-light images with the exclusively dark dataset," Computer Vision and Image Understanding, vol. 178, pp. 30-42, 2019.
[27] K. Ma, Z. Duanmu, H. Yeganeh and Z. Wang, "Multi-exposure image fusion by optimizing a Structural similarity index," IEEE Transactions on Computational Imaging, vol. 4, no. 1, pp. 60-72, 2018.
[28] C. Steffens, P. Lilles Jorge Drews and S. Silva Botelho, "Deep learning based exposure correction for image exposure correction with application in computer vision for robotics," 2018 Latin American Robotic Symposium, 2018 Brazilian Symposium on Robotics and 2018 Workshop on Robotics in Education, João Pessoa, Brazil, 2018, pp. 194-200.
[29] A. Mittal, A. K. Moorthy and A. C. Bovik, "No-reference image quality assessment in the spatial domain," IEEE Transactions on Image Processing, vol. 21, no. 12, pp. 4695-4708, 2012.
[30] K. Gu, D. Tao, J. F. Qiao and W. Lin, "Learning a no-reference quality assessment model of enhanced images with big data," IEEE Transactions on Neural Networks and Learning Systems, vol. 29, no. 4, pp. 1301-1313, 2018.